

Boundary-Layer Meteorol
 DOI 10.1007/s10546-012-9721-x

ARTICLE

Idealized Large-Eddy Simulations of Sea and Lake Breezes: Sensitivity to Lake Diameter, Heat Flux and Stability

Erik T. Crosman · John D. Horel

 Received: 30 May 2011 / Accepted: 15 March 2012
 © Springer Science+Business Media B.V. 2012

Abstract Idealized large-eddy simulations of lake and sea breezes are conducted to determine the sensitivity of these thermally-driven circulations to variations in the land-surface sensible heat flux and initial atmospheric stability. The lake-breeze and sea-breeze metrics of horizontal wind speed, horizontal extent, and depth are assessed. Modelled asymmetries about the coastline in the horizontal extent of the low-level onshore flow are found to vary as a function of the heat flux and stability. Small lake breezes develop similarly to sea breezes in the morning, but have a significantly weaker horizontal wind speed component and a smaller horizontal extent than sea breezes in the afternoon.

Keywords Lake breeze · Large-eddy simulation · Numerical modelling · Sea breeze · Thermally-driven circulation · Weather Research and Forecasting model

1 Introduction

Sea and large lake breezes have been studied extensively over the past several decades using observational and numerical approaches (Simpson 1994; Miller et al. 2003), and continue to be actively investigated (e.g., Levy et al. 2009; Papanastasiou et al. 2010; Soler et al. 2011). However, our understanding of these thermally-driven systems remains incomplete (see Crosman and Horel (2010) for a review of the numerical modelling of sea and lake breezes and recommendations for future research). Lake breezes for small lakes, however, have not been extensively studied and are not as well-understood as sea breezes (Segal et al. 1997). In this paper we describe initial findings from a numerical sensitivity study on sea and lake breezes concerning variations in the land-surface sensible heat flux, initial atmospheric stability, and lake diameter.

E. T. Crosman (✉) · J. D. Horel
 Department of Atmospheric Sciences, University of Utah, 135 S 1460 E Room 819 WBB,
 Salt Lake City, UT 84112-0110, USA
 e-mail: erik.crosman@utah.edu

As discussed by [Crosman and Horel \(2010\)](#), sea breezes have historically been studied in terms of three widely-used metrics: (1) the horizontal extent l , (2) the horizontal wind speed u , and (3) the depth h of these thermally-driven circulations. A number of scaling analyses using both observational and numerical data have been derived to approximate the environmental controls on these three sea-breeze metrics (e.g., [Niino 1987](#); [Dalu and Pielke 1989](#); [Steyn 1998, 2003](#); [Drobinski et al. 2006](#); [Porson et al. 2007](#)). In addition, a few scaling relations have attempted to characterize the differences between sea breezes and the smaller lake breezes and inland breezes resulting from land-surface heterogeneities (e.g., [Anthes 1984](#); [Segal et al. 1997](#); [Patton et al. 2005](#); [Courault et al. 2007](#); [Baldi et al. 2008](#); [Drobinski and Dubos 2009](#); [Hidalgo et al. 2010](#)).

Despite the abundance of sea-breeze modelling, scaling, and observational studies, no sensitivity study to our knowledge has modelled the three-dimensional structure of the sea-breeze circulation under a wide range of environmental forcing. In addition, no study has systematically modelled the differences in u , l , and h for small lake breezes versus larger lake and sea breezes. Several studies have noted the differing dynamics of sea and large lake breezes and small lake breezes and inland breezes ([Segal et al. 1997](#); [Drobinski and Dubos 2009](#)). Small lake breezes are fundamentally different from sea breezes due to the limited cool boundary-layer air available to the thermally-driven circulation and the limited extent offshore to which the competing mirror circulations can grow horizontally ([Crosman and Horel 2010](#)).

In this study we provide new insights into the detailed spatial and temporal characteristics of small lake breezes using large-eddy simulations (LES), where the larger-scale boundary-layer turbulence and the small-scale structure and frontal dynamics of the breezes are resolved. The ability of LES to realistically reproduce a single sea-breeze life cycle has been amply demonstrated ([Sha et al. 1991, 1993, 2004](#); [Dailey and Fovell 1999](#); [Rao et al. 1999](#); [Fovell and Dailey 2001](#); [Ogawa et al. 2003](#); [Fovell 2005](#)). [Antonelli and Rotunno \(2007\)](#) were the first to conduct numerical sensitivity studies concerning the sea-breeze onset using LES, and in this study we build on their work.

2 Model and Experiment Design

2.1 Weather and Forecasting Model Configuration

The National Center for Atmospheric Research (NCAR) Advanced Weather Research and Forecasting (WRF) model is a fully-compressible, non-hydrostatic atmospheric model ([Skamarock and Klemp 2008](#); [Skamarock et al. 2008](#)) that has been used extensively in LES ([Moeng et al. 2007](#); [Rotunno et al. 2009](#); [Catalano and Moeng 2010](#); [Lundquist et al. 2010](#)).

Details on the WRF model configured as a LES model for this study are given in Table 1. The model was run with a horizontal grid spacing of 100 m such that no planetary boundary-layer parametrization was required. In addition, because a dry atmosphere was assumed and surface fluxes were prescribed, no radiation, microphysical, or land-surface parametrizations were used. Surface drag was computed using Monin–Obuhkov similarity theory and subgrid-scale turbulence was modelled using a 1.5-order turbulent kinetic energy closure and the non-linear backscatter anisotropic turbulence subgrid-stress model of [Mirocha et al. \(2010\)](#).

The model domain for the WRF simulations follows the general approach of [Antonelli and Rotunno \(2007\)](#) (Fig. 1). The primary differences between our study and that of [Antonelli and Rotunno \(2007\)](#) are: the simulations reported herein (1) were run for a longer period of

Idealized Large-Eddy Simulations of Sea and Lake Breezes

Table 1 WRF model LES details

Model parameter	Model configuration (WRF namelist selections in italics)
Numerics	WRF Version 3.2, non-hydrostatic, Runge–Kutta 3rd order time-splitting time integration, 5th (3rd) order horizontal (vertical) momentum advection, stress mixing (<i>diff_opt = 2</i>)
Grid	Terrain-following hydrostatic-pressure (vertical) and Arakawa C-grid (horizontal)
Parametrizations	Obukhov surface layer (<i>sf_sfclay_physics = 1</i>), no radiation, PBL, or land-surface schemes; subgrid-scale turbulence: 1.5 order TKE (<i>km_opt = 2</i>) with NBA of Mirocha et al. (2010) (<i>sfs_opt = 2</i>)
Domain	230 km (<i>x</i>) × 5 km (<i>y</i>) × 5 km (<i>z</i>)
<i>x</i> -grid spacing	100 m (2,300 grid points)
<i>y</i> -grid spacing	100 m (65 grid points)
<i>z</i> -grid spacing	30–150 m stretched (65 grid points)
Boundary conditions	Periodic along-shore; open cross-shore
Timestep	1 s (acoustic timestep 0.166 s)
Simulation length	10 h
Damping	W-Rayleigh layer at model top (500 m deep), coefficient 0.1; numerical diffusion of Kniewel et al. (2007) (<i>diff_6th_factor = 1</i>)
Prescribed sensible heat flux	According to Eq. 1 over land, zero over water
Fixed initialization parameters	Initial land surface temperature 288.15 K, roughness length over land 0.2 m, roughness length over water 0.0001 m, Coriolis parameter (<i>f</i>) = 10 ⁻⁴ s ⁻¹ , initial geostrophic flow zero (<i>H</i> , K m s ⁻¹) = 0.16; (<i>N</i> , s ⁻¹) = 0.01
CTL simulation	
Heat flux sensitivity tests	(<i>H</i> , K m s ⁻¹) = 0.08 (<i>LO_H</i>); 0.16 (CTL); 0.30 (<i>HI_H</i>)
Initial stability sensitivity test	(<i>N</i> , s ⁻¹) = 0.005 (<i>LO_N</i>); 0.01 (CTL); 0.02 (<i>HI_N</i>)
Lake diameter sensitivity tests	(<i>d</i> , km) = 10 (<i>LK_10</i>); 25 (<i>LK_25</i>); 50 (<i>LK_50</i>); 100 (<i>LK_100</i>); sea (infinite dimension)

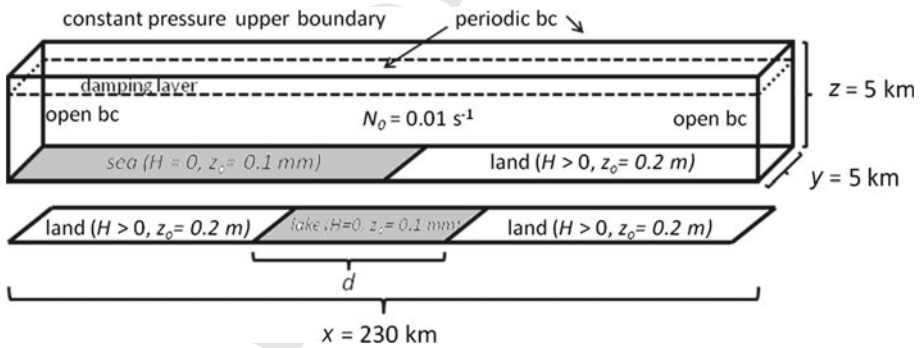


Fig. 1 Schematic diagram of simulation set-up for control sea-breeze simulation (Table 1) (top) and lake-breeze cases (bottom). *H* represents the land-surface sensible heat flux, *N*₀ is the initial Brunt–Viasala frequency, *z*₀ is the roughness length, and *d* is the lake diameter

67 time over a greater horizontal domain (10 h versus 6 h; 230 km versus 100 km), (2) included
68 a time-varying land-surface sensible heat flux (instead of fixed), (3) included idealized lake
69 surfaces, and (4) were conducted over a larger range of the land-surface sensible heat flux
70 and initial atmospheric stability. The model was run in three dimensions, with a volume of
71 dimension 5 km along-coast (y) \times 230 km cross-coast (x) \times 5 km vertical (z). Assuming a
72 straight coastline parallel to y results in two-dimensional sea-breeze circulations in the x - z
73 plane while simulating the three-dimensionality of individual convective eddies. Periodic
74 boundary conditions were imposed in the y -direction with open boundary conditions in the
75 x -direction. The model was run with a 100-m grid resolution in x and y , and a stretched z
76 grid ranging from ≈ 30 m at the lowest level to ≈ 150 m below the model top (Crosman 2011).
77 A damping layer was used at the model top to avoid the reflection of acoustic and gravity
78 waves. The model was run for 10 h using a 1-s timestep (Table 1). The surface boundary
79 conditions were partitioned between land and water (lake or sea) surfaces (Fig. 1). The land-
80 surface sensible heat flux was set to zero over the sea or lake surface, while over the land
81 surface a time-varying land-surface sensible heat flux (H) was prescribed by

$$82 \quad H(t) = A \sin \left[\left(\frac{\pi}{12} \right) \left(\frac{t}{3600} \right) \right] \quad (1)$$

83 where t is the time in seconds from model initialization and A is the heat-flux amplitude.
84 The aerodynamic roughness length was prescribed as 0.0001 m over water and 0.2 m over
85 land (Table 1). The transition between the water and land surfaces was modelled with a 300
86 m gradient in both the surface heat flux and drag. The initial surface temperature was 288.15
87 K, there was no initial geostrophic flow, and the Coriolis parameter was set to 10^{-4} s^{-1} . The
88 initial atmospheric stability profiles were prescribed to be horizontally homogeneous over
89 land and water.

90 2.2 Sensitivity Tests

91 Twenty-five LES were conducted on the sensitivity of the horizontal cross-coast wind speed
92 u , inland extent l of the sea-breeze or lake-breeze front from the coast, and depth h (at the
93 coast unless noted otherwise) of sea and lake breezes to the land-surface sensible heat flux (H ,
94 referred to hereafter as “heat flux”) and the initial atmospheric stability (N , referred to here-
95 after as “stability”) (Table 1). Various combinations of the three different values of the peak
96 amplitude A of the heat flux ($H = 0.08, 0.16, 0.30 \text{ K m s}^{-1}$) and stability (Brunt–Viasala
97 frequency $N = 0.005, 0.01, 0.02 \text{ s}^{-1}$) were prescribed in the simulations of four slab-sym-
98 metric (i.e., an elongated lake with two-dimensional symmetry) lakes with diameters of 10,
99 25, 50 and 100 km and the ‘infinite’ sea-breeze dimension (Table 1).

100 The range of heat fluxes used corresponds roughly to low ($\approx 90 \text{ W m}^{-2}$), medium (≈ 180
101 W m^{-2}), and high ($\approx 375 \text{ W m}^{-2}$) environmental values (Hsu 1983). The range of stability
102 used also corresponds roughly to a low-stability (0.005 s^{-1}), standard-stability (0.01 s^{-1})
103 or high-stability (0.02 s^{-1}) atmosphere. In the low-stability atmosphere, the boundary layer
104 over the land surface mixes to near-neutral in the presence of the high heat flux, representing
105 the case of a sea breeze forming in an arid coastal region. Conversely, the high-stability
106 atmosphere (0.02 s^{-1}) would be more representative of a sea breeze forming under a capping
107 inversion, possibly resulting from a pre-existing nocturnal inversion, marine boundary layer,
108 or elevated stable layer.

109 This study has several limitations that should be noted. First, because there is no land-
110 surface model and the heat fluxes are prescribed in time according to Eq. 1, the model does
111 not simulate interactions between the cool onshore flow and ground temperature. Second,

112 the heat flux in this study is set to zero over water surfaces although small negative values
113 are typically observed due to evaporative cooling (Segal et al. 1997). Third, homogeneous
114 initial atmospheric conditions were assumed over the land and water surfaces. Fourth, the
115 simulations were terminated after 10 h (mid-afternoon) to avoid numerical instabilities occa-
116 sionally observed at the lateral boundaries after that time. Finally, the modelling framework
117 (i.e., quasi-two-dimensional) for lakes in this study does not allow for consideration of coast-
118 line curvature effects.

119 For the purposes of the study, time will be given in hours from the start of a simulation.
120 Thus, hr 6 corresponds to noon local solar time, with hr 10—the end of the simulation—cor-
121 responding to mid-afternoon. References to ‘morning’ indicate times prior to simulation hr
122 6, whereas ‘afternoon’ refers to simulation hrs 6–10.

123 3 Results and Discussion

124 3.1 Control Simulation

125 The overall development of the sea breeze in the control (CTL) run is consistent with pre-
126 vious observational and numerical studies (Reible et al. 1993; Miller et al. 2003; Bastin and
127 Drobinski 2006). The sea-breeze circulation initiates near the coast and expands laterally
128 and vertically during the daytime life cycle (Fig. 2a–c). During the morning, the region of
129 low-level onshore flow with horizontal wind speeds $>2 \text{ m s}^{-1}$ is confined to within 10 km of
130 the coast (Fig. 2a), and by mid-afternoon the region of low-level onshore flow with horizontal
131 wind speeds $>4 \text{ m s}^{-1}$ has extended onshore and offshore by over 30 km (Fig. 2c). An after-
132 noon maximum in the cross-coast wind speeds associated with the sea-breeze return flow
133 is noted behind the sea-breeze front between 1 and 2 km above the surface. The horizontal
134 temperature gradient between the coast and the leading edge of the sea-breeze front (≈ 38
135 km inland at hr 9) increases from $\approx 2 \text{ K}$ at hr 3 to $\approx 4 \text{ K}$ by hr 9. The competing effects of
136 turbulent convection, which acts to deepen the internal marine boundary layer (Garratt 1990),
137 and the stable marine onshore flow, which limits the sea-breeze depth are evident. The sea-
138 breeze low-level onshore flow deepens and becomes increasingly turbulent with increasing
139 distance inland during the afternoon (Fig. 2b, c). The sea-breeze low-level onshore flow at the
140 coast remains a relatively constant depth ($\approx 600 \text{ m}$) through the afternoon, while the depth
141 of the low-level onshore flow immediately behind the sea-breeze front increases to >900
142 m (Fig. 2b, c). Vertical motions associated with the sea-breeze front and boundary-layer
143 convection ahead of the front also increase during the afternoon (Fig. 2b, c).

144 A general weakening of the low-level horizontal temperature gradient through turbulent
145 frontolysis is noted with increasing distance inland (the horizontal temperature gradient near
146 the coast is $\approx 0.25 \text{ K km}^{-1}$ as compared to $\approx 0.10 \text{ K km}^{-1}$ 25 km inland at hr 9). The sea-
147 breeze horizontal wind speeds increase linearly during the morning before levelling off in
148 the afternoon at the coast (Fig. 2d). Similar conditions are observed offshore over the ocean,
149 except that the horizontal wind speeds are smaller until hr 8 when the stronger core of the
150 low-level onshore flow has expanded sufficiently to reach that location. Inland from the coast
151 (4 km), a sea-breeze frontal passage is evident near hr 3, marked by an increase in the hori-
152 zontal wind speeds, and a flattening of the temperature trace (Fig. 2d, e). Further inland (24
153 km), the sea-breeze frontal passage is delayed until hr 7, which allows for greater diurnal
154 heating of the prefrontal boundary layer and development of the sea-breeze front, with an
155 associated 1.5 K temperature decrease associated with frontal passage.

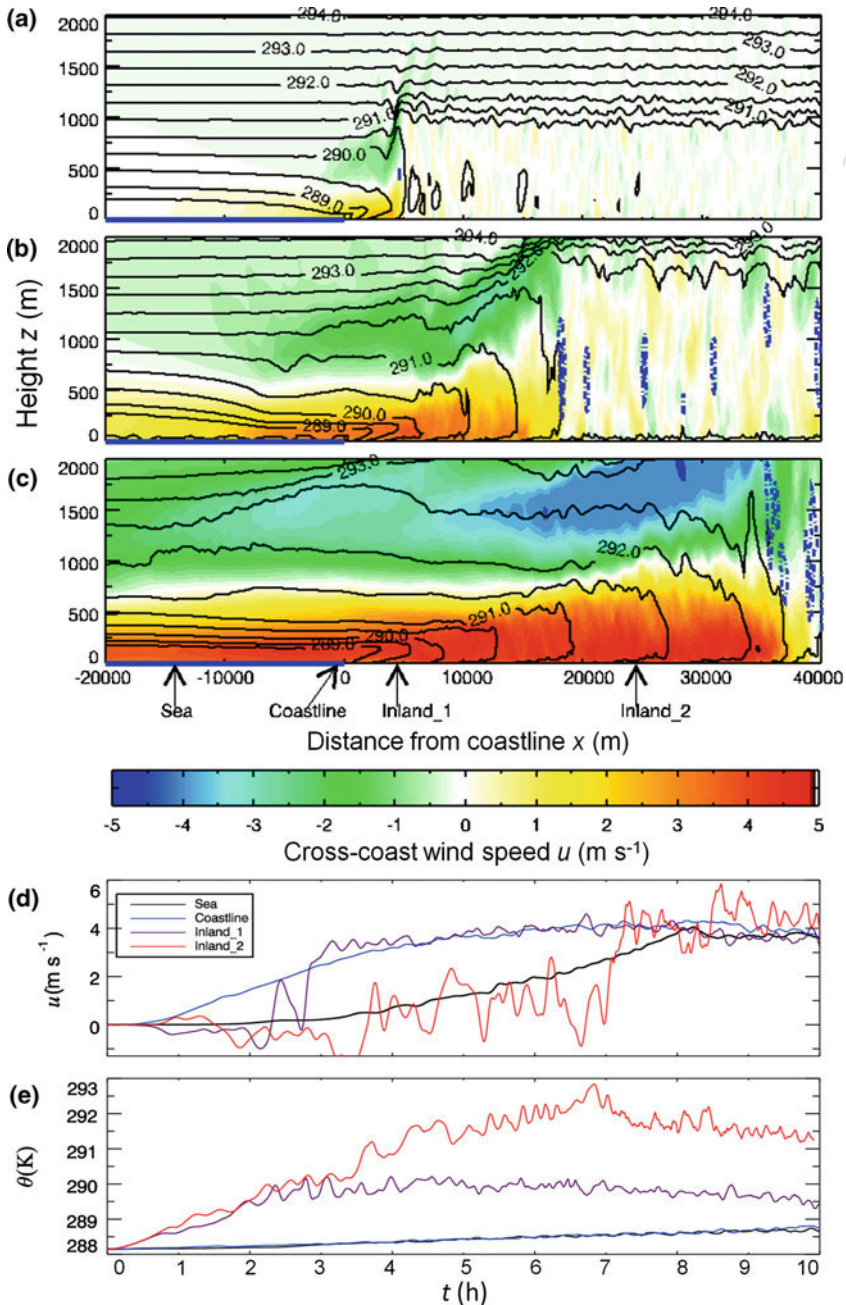


Fig. 2 a–c Vertical cross-sections of the y -averaged sea-breeze circulation for the CTL simulation (see Table 1) at hr a 3, b 6, and c 9 (time is hours after simulation start, i.e., sunrise). Colours represent the cross-coast wind speed (u , m s^{-1}) and solid contours represent potential temperature (θ , K). Regions of upward vertical motion greater than 0.5 m s^{-1} are contained within the dashed blue line. The sea surface is represented by solid blue line. The approximate locations of near-surface time series of d cross-coast wind speed u (m s^{-1}) and e potential temperature θ (K) are indicated with arrows in c

156 3.2 Sensitivity to the Land-Surface Sensible Heat Flux and Atmospheric Stability

157 In this section we summarize the effects of variations in the heat flux and stability on the
 158 structure of mature (mid-afternoon) sea-breeze and small lake-breeze ($d = 25$ km, hereafter
 159 referred to as lake unless otherwise noted) circulations. Several new findings on sea and lake
 160 breezes not previously reported in the literature are observed. First, horizontal asymmetries
 161 in the wind speed of the lake-breeze and sea-breeze onshore low-level flows are observed as a
 162 function of the heat flux and stability (Figs. 3, 4). Second, the highest wind speeds associated
 163 with the lake-breeze onshore low-level flow are noted immediately inland from the coastline
 164 (Figs. 3c, d; 4c, d). Other lake-breeze and sea-breeze responses to variations in the heat flux
 165 and stability are generally as expected: the horizontal cross-coast wind speed (for both the
 166 low-level onshore flow and the return flow aloft), vertical wind speed, circulation width,
 167 land-water temperature contrast, and depth of the lake and sea breezes in a high heat-flux
 168 environment generally increase relative to a low heat-flux environment (Fig. 3a–d), while
 169 a high stability atmosphere significantly decreases the depth of both the low-level onshore
 170 flow and the return flow aloft, in addition to damping the near-surface horizontal and vertical
 171 wind speeds (Fig. 4a–d). Relatively weak sea-breeze fronts are evident in the simulations,
 172 consistent with a lack of background flow to drive frontogenesis (Reible et al. 1993). The
 173 thermodynamic effects of variations in the heat flux are small near the shore since the increase
 174 in heating is largely offset by increased advection of marine air inland. Consequently, the
 175 near-shore surface temperature is similar for low and high surface heat fluxes, with the sur-
 176 face temperature 20 km inland from the coast ≈ 2 K higher in the high heat-flux environment
 177 (Fig. 3a, b).

178 3.2.1 Asymmetry of the Lake-Breeze and Sea-Breeze Circulations

179 For sea breezes, the region of maximum wind speeds associated with the onshore low-level
 180 flow is notably more asymmetric about the coastline for the low heat-flux and high stability
 181 cases (Figs. 3a, 4b) than for high heat-flux and low stability simulations (Figs. 3b, 4a). In
 182 the low heat flux and high stability cases, the horizontal extent of maximum wind speeds
 183 associated with the sea-breeze low-level onshore flow is approximately twice as far onshore
 184 as offshore (Figs. 3a, 4b). For the high heat-flux and low stability cases, the horizontal extent
 185 of maximum wind speeds within the sea-breeze low-level onshore flow is comparable in the
 186 onshore and offshore directions (Figs. 3b, 4a). For lake breezes, the offshore extent of the
 187 circulation is constrained to the middle of the lake due to the competing mirror circulations
 188 forming on either side of the water body. Thus, the lake breeze becomes increasingly asym-
 189 metric with increasing inland extent of the circulation. In the low stability and high heat-flux
 190 environments the inland extent of the lake breeze low-level onshore flow is roughly twice the
 191 offshore extent (Figs. 3d, 4c). In addition, the strongest lake-breeze horizontal wind speeds
 192 within the low-level onshore flow are generally observed within 10 km inland from the coast
 193 for both low and high heat-flux and stability environments (Figs. 3c, d; 4c, d).

194 In addition to the noted asymmetry in the horizontal extent of the low-level onshore flow,
 195 the overall horizontal shape of the lake-breeze and sea-breeze circulations is also asymmetric
 196 about the coast, with the low-level onshore flow observed to be deeper and to have a higher
 197 vertically-averaged horizontal wind speed over the land than over the sea. The horizontal
 198 wind speed of the return flow is also notably stronger over the land than over the sea (Figs. 3,
 199 4). These findings are consistent with the observations of Drobinski et al. (2006) who found
 200 that sea-breeze circulations were “far from the toroidal circulation found in the textbooks.”

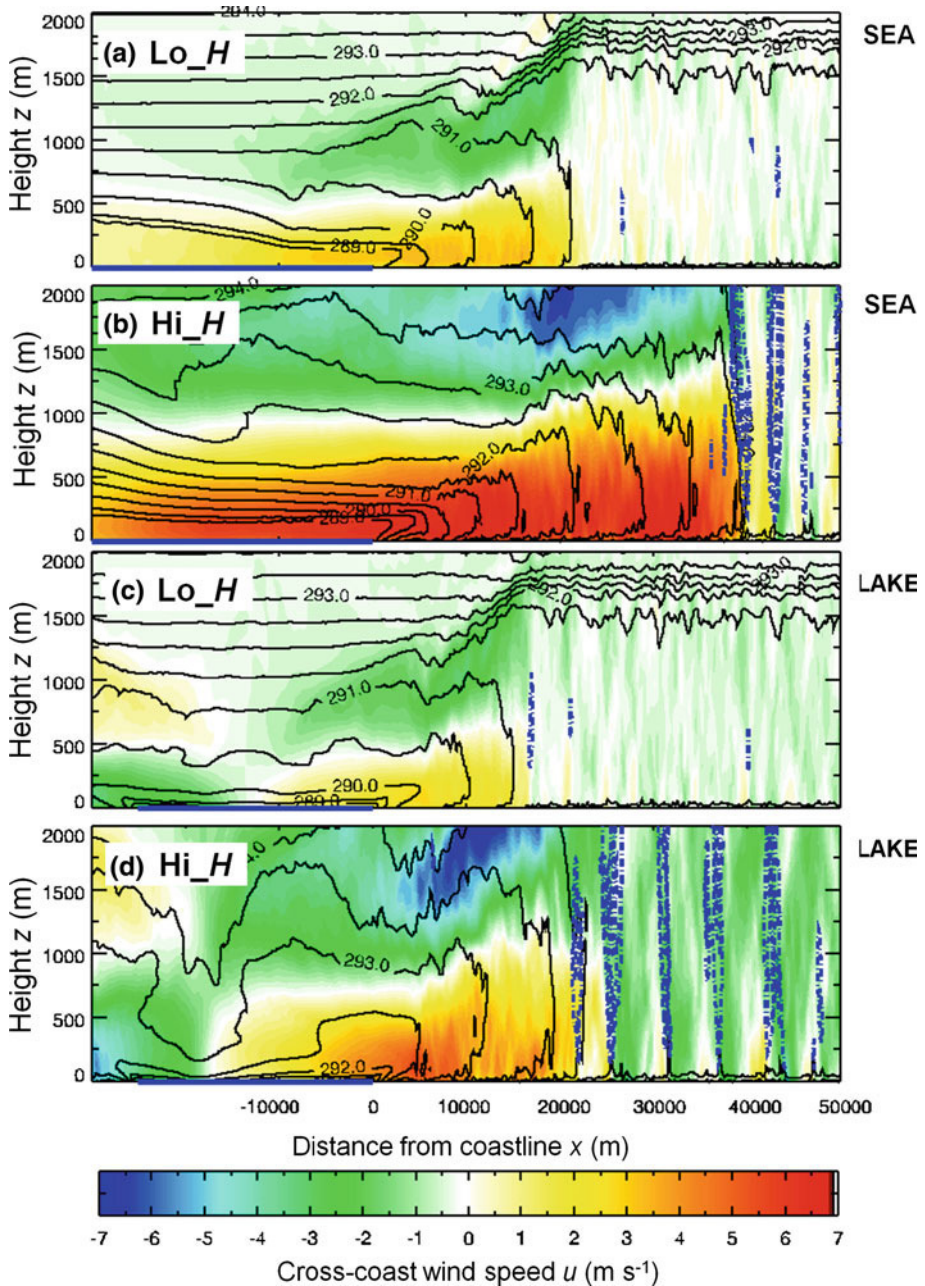


Fig. 3 Vertical cross-section of the y -averaged circulations at hr 8 (time is hours after simulation start) for experiments **a** LO_H and **b** HI_H for the sea-breeze case and **c** LO_H and **d** HI_H for a 25 km lake. Colours represent the cross-coast wind speed (u , m s^{-1}) and solid contours represent potential temperature (θ , K). Regions of upward vertical motion greater than 0.5 m s^{-1} are contained within the dashed blue line. The sea or lake surfaces are represented by solid blue lines

Idealized Large-Eddy Simulations of Sea and Lake Breezes

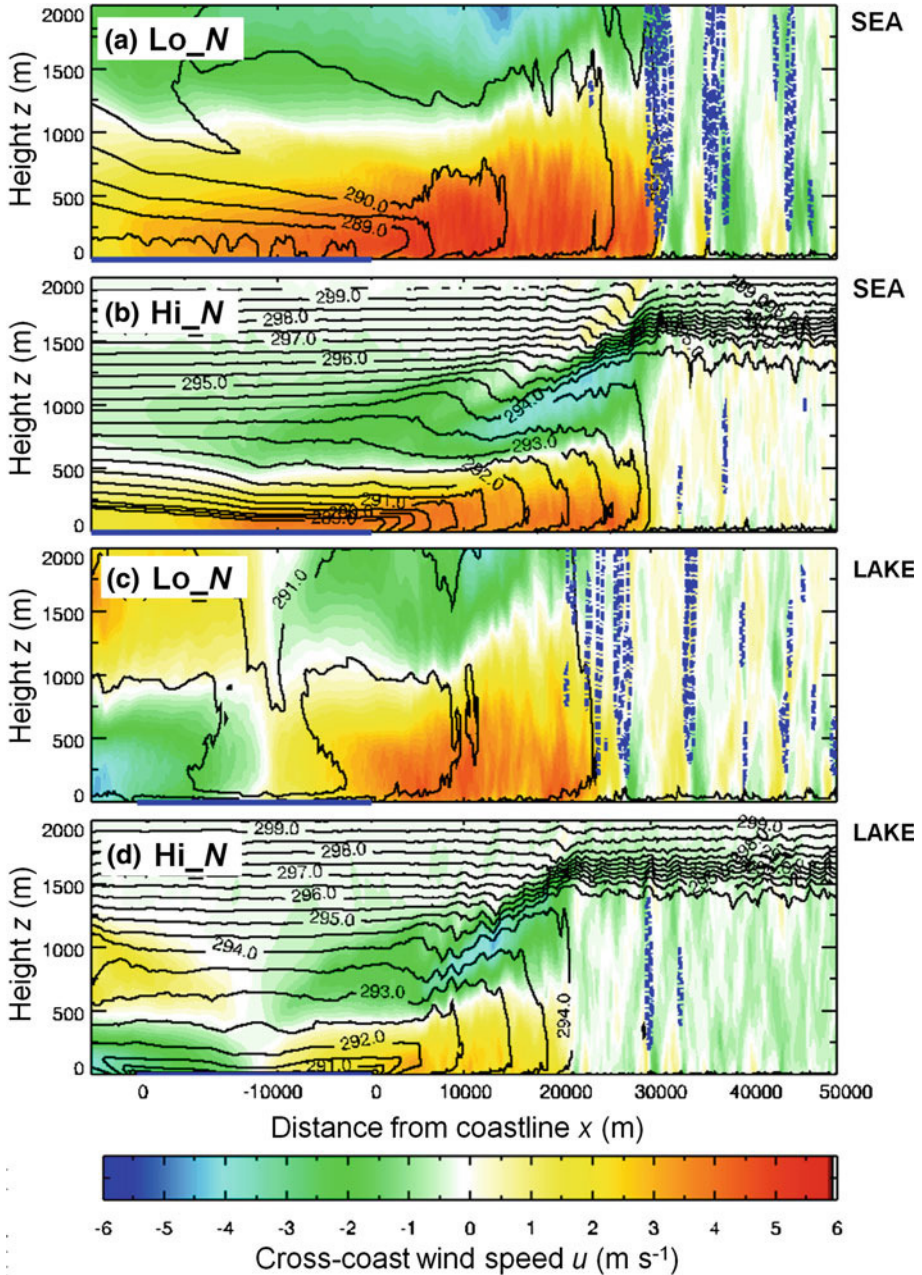


Fig. 4 Vertical cross-section of the y -averaged circulations at hr 8 (time is hours after simulation start) for experiments **a** LO_N and **b** HI_N for the sea-breeze case and **c** LO_N and **d** HI_N for a 25 km lake. Colours represent the cross-coast wind speed (u , m s^{-1}) and *solid contours* represent potential temperature (θ , K). Regions of upward vertical motion greater than 0.5 m s^{-1} are contained within the *dashed blue line*. The sea or lake surfaces are represented by *solid blue lines*

201 *3.2.2 Difference Between Lake-Breeze and Sea-Breeze Circulations*

202 Lake-breeze circulations are expected to be smaller and weaker than the corresponding sea-
 203 breeze circulations (Segal et al. 1997). The LES of the lake breezes have decreased horizontal
 204 cross-coast wind speeds and a smaller horizontal extent compared to the corresponding sea
 205 breezes (Figs. 3, 4). First, the difference between the lake-breeze and sea-breeze inland extent
 206 increases with increasing heat flux (Fig. 3). Second, the highest observed wind speeds in the
 207 low-level onshore flow and horizontal temperature gradients associated with lake breezes are
 208 limited to the near-shore environment, while sea breezes have larger temperature gradients
 209 and wind speeds in the onshore low-level flow that extends further inland (Figs. 3, 4). The
 210 low-level horizontal temperature gradient associated with the small lake breeze also remains
 211 relatively invariant with increasing heat flux (Fig. 3c, d). Finally, lake breezes appear to be
 212 more sensitive to variations in stability than sea breezes, as the differences between lake-
 213 breeze low-level onshore flow wind speeds, inland extent, and depth between high and low
 214 stabilities are larger than the relative changes in sea breezes between high and low stabilities
 215 (Fig. 4a–c). A physical hypothesis for some of these differences will be discussed in Sect. 3.5.

 216 *3.3 Temporal Dependence*

217 The temporal evolution of the lake-breeze and sea-breeze horizontal wind speeds at the coast,
 218 inland extent, and depth of the low-level onshore flow at the coast for five different environ-
 219 nments is given in Fig. 5. The sea-breeze horizontal wind speed, inland extent, and depth in
 220 a high heat-flux environment is approximately twice that observed in a low heat-flux envi-
 221 ronment (Fig. 5a, c, e). For a low heat flux, the horizontal wind speed increases through late
 222 morning and remains relatively constant during the afternoon. For a medium and high heat
 223 flux, the sea-breeze horizontal wind speed increases through early afternoon before decreas-
 224 ing. The inland penetration speed of the sea-breeze front (i.e., the time rate of change of the
 225 inland extent of the sea breeze) is also sensitive to the heat flux. For a low heat flux, the inland
 226 penetration speed is $\approx 5 \text{ km h}^{-1}$ during the entire simulation (Fig. 5c). For the medium and
 227 high heat fluxes, there is a notable afternoon increase in the inland penetration speed to 7.5
 228 and 10 km h^{-1} respectively. These values qualitatively agree with the observed inland penetra-
 229 tion speeds of $3\text{--}5 \text{ km h}^{-1}$ ($6\text{--}8 \text{ km h}^{-1}$) modelled by Tijn (1999) and Physick (1980) for
 230 low (high) heat-flux environments, as well as the sea-breeze observations of Simpson (1994)
 231 and Bastin and Drobinski (2006). In addition, several studies have confirmed the afternoon
 232 acceleration of the sea-breeze front (Physick 1980; Ogawa et al. 2003). The lake-breeze and
 233 sea-breeze horizontal wind speeds are insensitive to stability until hr 5, after which point
 234 a weak dependency on stability exists (Fig. 5a, b). The inland extent of sea breezes is vir-
 235 tually independent of stability (Fig. 5c), while the lake-breeze and sea-breeze depths vary
 236 significantly as a function of stability (Fig. 5e, f).

 237 *3.3.1 Comparison with Sea-Breeze Scaling Estimates*

238 Figure 6 summarizes the changes in the three key metrics (u , h , and l) at mid-afternoon
 239 resulting from doubling the heat flux and stability in the LES. The impact of doubling those
 240 quantities (i.e., from low to medium and medium to high as defined in Table 1) are expressed
 241 in terms of the fractional change in the breeze metrics to 100 % increases in the magnitudes
 242 of the heat flux and stability. For example, the cross-coast horizontal wind speed at the coast
 243 in the sea-breeze LES increases by 50 % when the heat flux is increased from low to medium
 244 with roughly similar increases found when the heat flux is doubled again (Fig. 6a). Also shown

Idealized Large-Eddy Simulations of Sea and Lake Breezes

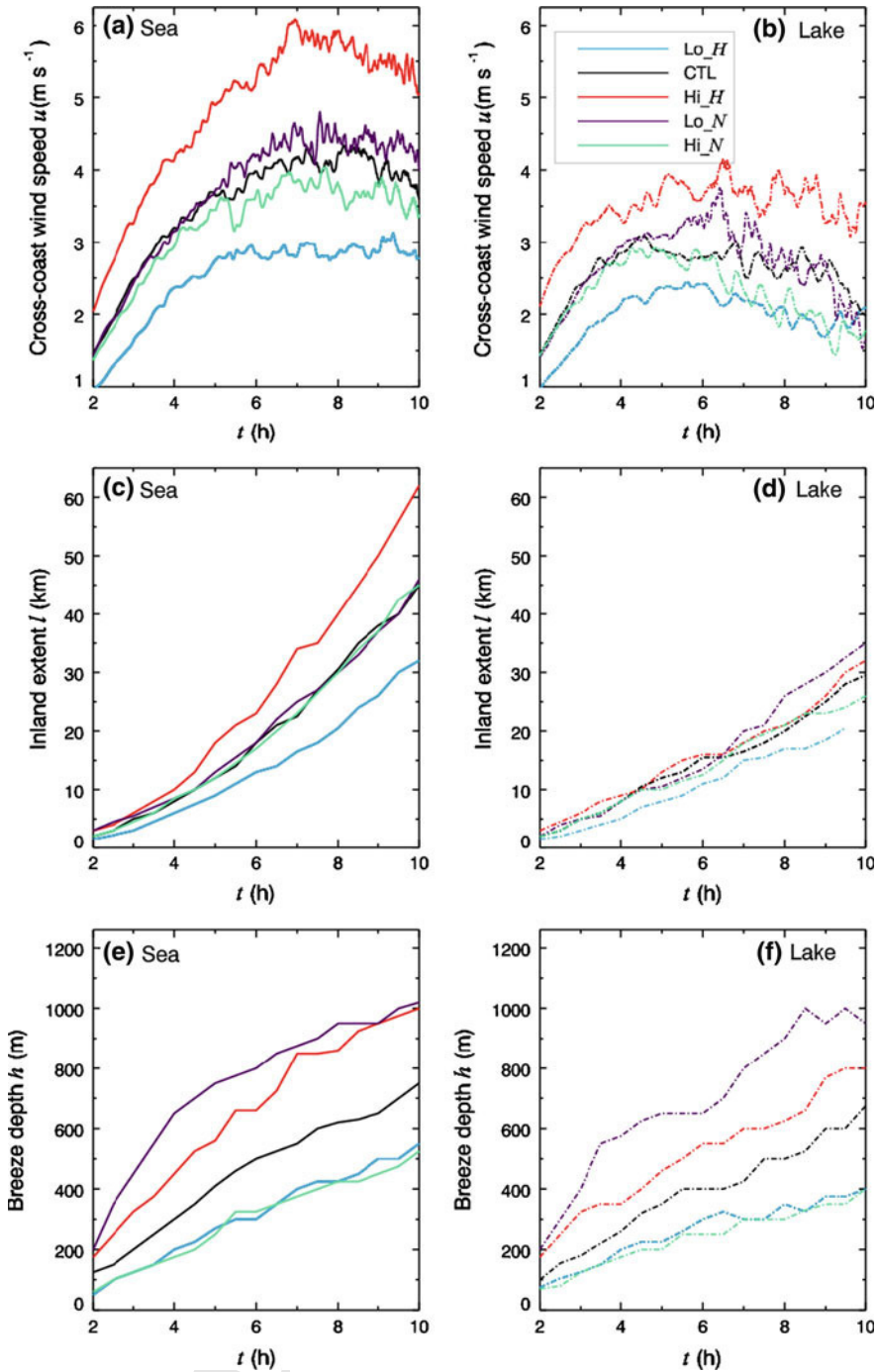


Fig. 5 Time series of **a, b** cross-coast wind speed u (m s^{-1}) at the coast (30 m a.g.l.), **c, d** inland extent l (km), and **e, f** depth h (m) at the coast for low, medium, and high values of the land-surface sensible heat flux and initial atmospheric stability (see Table 1 for more info). **a, c** and **e** refer to sea-breeze simulations while **b, d** and **f** refer to a 25-km diameter lake. Time on the *horizontal* axis refers to hours after simulation start

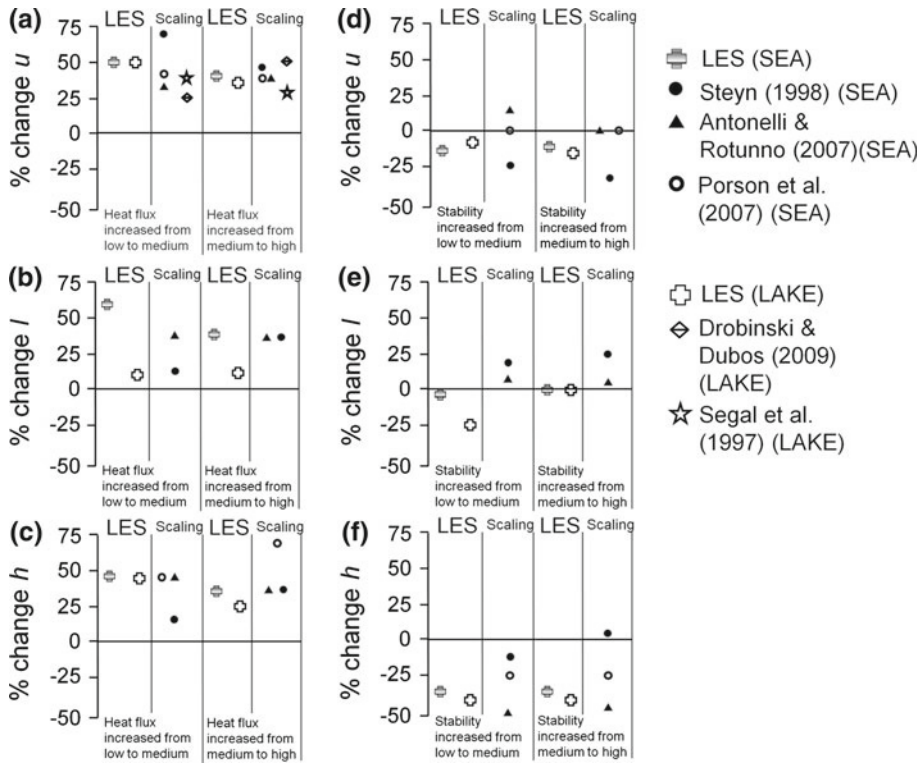


Fig. 6 Impact of a 100 % increase in the heat flux and stability (from low to medium and from medium to high values) on the mature mid-afternoon (hr 8) sea-breeze and lake-breeze circulations as observed in sea-breeze and 25-km diameter lake-breeze LES as well as according to several widely-used scaling estimates. **a** and **d** Cross-coast wind speed u (m s^{-1}), **b** and **e** inland extent l (km), and **c** and **f** depth h (m) expressed as the fractional change (change divided by original value)

in Fig. 6 are estimates of the changes in these metrics expected from multiple scaling relations developed for sea and lake breezes. The scaling technique is outlined by Steyn (1998) and reviewed by Crosman and Horel (2010). In general, the sea-breeze scaling relations appear to capture the LES' response to variations in the heat flux and stability. A doubling of the heat flux results in substantial increases in the sea-breeze horizontal wind speed, depth, and inland extent (Fig. 6a–c). A doubling of the stability results in small changes in the sea-breeze horizontal wind speeds and inland extent and large decreases in depth (Fig. 6d–f).

However, there are several notable discrepancies between the LES and the scaling estimates. These discrepancies bring into question the 'universality' of these scaling laws for the wide range of environments simulated. The scaling estimates for changes in depth with variations in stability by Steyn (1998) and Porson et al. (2007) are less than those of Antonelli and Rotunno (2007) and the LES in this study (Fig. 6f). The Steyn (1998) scaling estimates for the horizontal wind speed and inland extent also disagree with the model simulations in several instances, possibly due to the use of an instantaneous rather than integrated heat flux used in the Steyn (1998) scaling estimates (Drobinski et al. 2006).

Finally, the scaling relations for inland (Drobinski and Dubos 2009) and lake (Segal et al. 1997) breezes for the horizontal wind speed are examined for the 25-km lake LES (Fig. 6a).

Idealized Large-Eddy Simulations of Sea and Lake Breezes

262 The inclusion of lake diameter in the scaling for wind speed appears to be of secondary
263 importance relative to the heat flux, which is further supported by the similar sensitivities
264 to heat flux between the lake and sea LES. However, scaling estimates of the inland extent
265 should depend on lake diameter since the lake-breeze and sea-breeze horizontal length scales
266 respond differently to increases in heat flux and to a lesser extent stability (Fig. 6b, e).

267 *3.3.2 Difference Between the Lake-Breeze and Sea-Breeze Evolution*

268 The horizontal wind speed, inland extent, and depth of small lake breezes in many cases show
269 similar sensitivities to variations in the heat flux and stability as for sea breezes (Fig. 5b, d,
270 f). However, there are some notable differences between lake breezes and sea breezes:

- 271 • the lake-breeze characteristics are similar to sea breezes through mid-morning;
- 272 • the afternoon lake-breeze horizontal wind speed and inland extent are significantly less;
- 273 • there is no inland acceleration of the lake-breeze front in the afternoon;
- 274 • the lake-breeze inland extent is less sensitive to the heat flux;
- 275 • the relative decrease in lake-breeze depth with respect to the sea breeze is less than the
276 relative decrease in the horizontal wind speed and inland extent.

277 A discussion of possible reasons for some of these differences is given in Sect. 3.5.

278 *3.4 Sensitivity to Lake Diameter*

279 The analysis to this point has focused on a comparison of sea breezes with a 25-km diam-
280 eter lake. A natural question that follows from this discussion is: how does the comparison
281 between sea and lake breezes vary as the lake size is changed? It is generally agreed that for
282 large lakes ($d = 100$ km), the lake-breeze characteristics are similar to those for sea breezes,
283 and the results of our study confirm this (Fig. 7). A comparison of the LES lake-breeze evo-
284 lution for a large lake (Fig. 7a–c) with [Keen and Lyons \(1978\)](#) Lake Michigan breeze shows
285 similar horizontal wind speeds (≈ 4 m s⁻¹) and depths (≈ 500 – 800 m).

286 However, the horizontal wind speed, inland extent, and depth of lake breezes are observed
287 to decrease with decreasing lake diameter for small- to medium-sized lakes, $d = 10$ – 50 km
288 (Fig. 7a–c). The sensitivity of these lake-breeze metrics to lake diameter is highest in the
289 afternoon. Through mid- to late morning, the horizontal wind speed, inland extent, and depth
290 of lake breezes (except for the smallest case $d = 10$ km) show virtually no dependence on
291 lake diameter (Fig. 7).

292 The response of lakes breezes to variations in the heat flux and stability is also modulated
293 by the lake diameter (Fig. 7d–f). The mid-afternoon horizontal wind speed and inland extent
294 of medium and large lakes are more sensitive to variations in the heat flux than small lakes.
295 The difference in horizontal wind speed and inland extent between lake breezes for small and
296 large lakes is highest for a high heat-flux environment (Fig. 7d, e). For example, the difference
297 in lake-breeze horizontal wind speed between small and large lakes is ≈ 1.5 m s⁻¹ under a
298 low heat flux and increases to ≈ 4 m s⁻¹ for a high heat flux. Similarly, the inland extent of
299 small and large lakes differs by ≈ 6 km under low heat-flux conditions and increases to ≈ 17
300 km under high heat-flux conditions. For a low heat flux, the lake-breeze depth is relatively
301 insensitive to lake size, while for a medium and high heat flux, the depth is dependent on the
302 lake diameter (Fig. 7f). Variations in stability weakly modulate the response of lake breezes
303 to lake diameter (Fig. 7d–f). The relative differences in horizontal wind speed, inland extent,
304 and depth for lake breezes between 10- and 50-km diameter lakes are greater in a low stability
305 environment than a high stability environment.

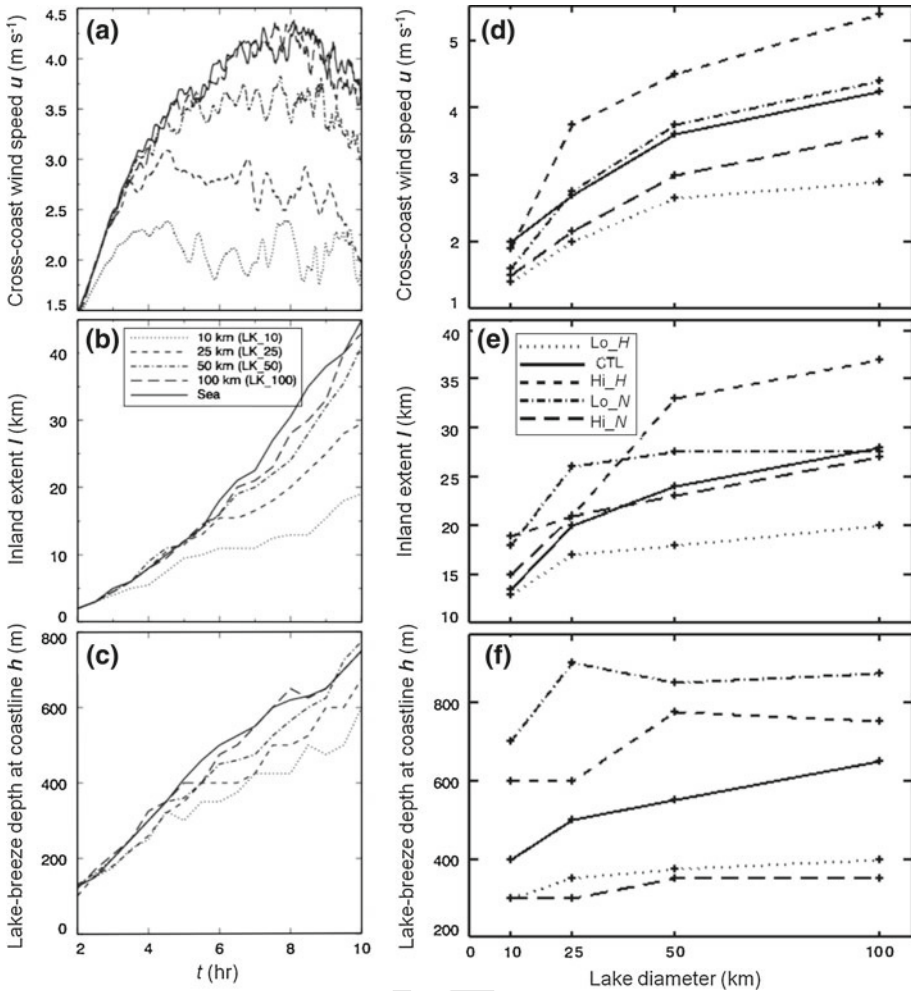


Fig. 7 Lake-breeze and sea-breeze **a** cross-coast wind speed u (m s^{-1}) at the coast (30 m a.g.l.), **b** inland extent l (km), and **c** depth h (m) at the coast for lakes of diameter 10, 25, 50 and 100 km and the sea-breeze case. Time on the *horizontal axis* refers to hours after simulation start. The sensitivity of **d** u , **e** l , and **f** h as a function of lake diameter at simulation hr 8 for low, medium, and high values of the land-surface sensible heat flux and initial atmospheric stability

306 3.4.1 Variations in the Lake-Breeze and Sea-Breeze Aspect Ratios

307 Motivated by the comparison of sea-breeze and inland-breeze aspect ratios (inland
 308 extent/depth) reported by [Drobinski and Dubos \(2009\)](#), we provide a brief overview of the
 309 modelled lake-breeze and sea-breeze aspect ratios as a function of lake diameter, heat flux,
 310 and stability. The 10-, 25- and 50-km diameter lakes in this study are likely in the ‘transi-
 311 tional regime’ between very small land-surface heterogeneities and sea breezes ([Drobinski
 312 and Dubos 2009](#)). Similar to the findings of [Drobinski and Dubos \(2009\)](#), the aspect ratio is
 313 smaller for small lake breezes than for sea breezes (Fig. 8). The modelled sea-breeze aspect
 314 ratios are lower than those observed by [Drobinski et al. \(2006\)](#) because the inland extent

Idealized Large-Eddy Simulations of Sea and Lake Breezes

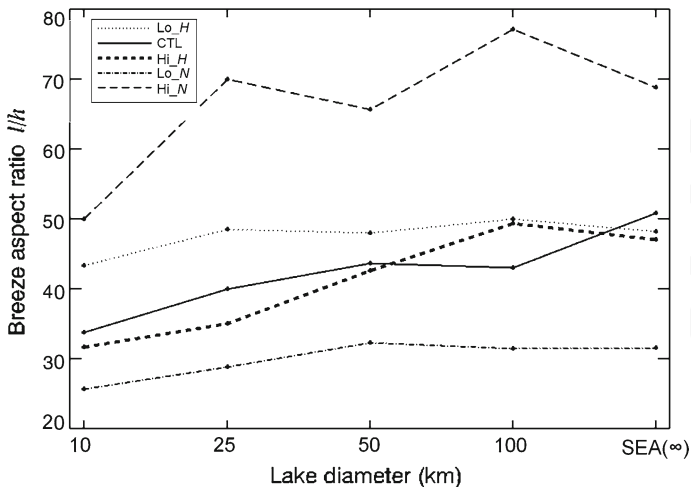


Fig. 8 Aspect ratio (inland extent l divided by depth h at the coast) of sea-breeze and lake-breeze circulations observed at mid-afternoon (hr 8) for low, medium, and high values of the land-surface sensible heat flux and initial atmospheric stability

315 is computed at mid-afternoon rather than in early evening when the sea-breeze front has
 316 progressed further inland. The aspect ratio at mid-afternoon is observed to vary strongly as
 317 a function of the land-surface sensible heat flux and stability. For a low stability atmosphere
 318 the aspect ratio is much smaller than for a high stability atmosphere. For a low land-surface
 319 heat flux, the aspect ratio is relatively uniform for all lake diameters, while the sea-breeze
 320 aspect ratio for a high land-surface heat flux is over 50 % greater than that of a lake breeze
 321 associated with a 10-km diameter lake.

322 3.5 Physical Mechanisms Influencing Lake Breezes

323 Two physical mechanisms are known to weaken lake breezes relative to sea breezes. First,
 324 there is a limited supply of cool air available over the lake for the developing lake-breeze
 325 circulations, and second, the lake-breeze circulations around the lake compete for the avail-
 326 able cool air and horizontal space in which to grow laterally offshore (Crosman and Horel
 327 2010). In addition, for a small lake with a diameter of a few km, surface friction becomes
 328 increasingly important in the breeze dynamics (Drobninski and Dubos 2009).

329 The comparison of small lake and sea breezes to this point has shown that, in the morning,
 330 lake-breeze circulations associated with small lakes are typically similar to sea breezes while
 331 in the afternoon small lake breezes have weaker winds speeds in the low-level onshore flow
 332 and lake-breeze fronts that do not penetrate inland as rapidly as sea-breeze fronts. In addition,
 333 the strongest lake-breeze low-level onshore flow and horizontal temperature gradients have
 334 been shown to remain fixed near the coast and not extend inland as in the case of a sea breeze.

335 An analysis of the LES shows that the depletion of cool air over small and medium-sized
 336 lakes and the limiting offshore extent for the lake-breeze circulations to expand horizontally
 337 influence the evolution of the lake breeze. Because of a combination of depletion of the cool
 338 air over the lake and subsidence warming at the intersection of the two lake-breeze circu-
 339 lations in the centre of the lake, the boundary layer over the lake surface in the afternoon
 340 is much warmer than that over the sea (Fig. 9). The warming of the lake boundary layer by

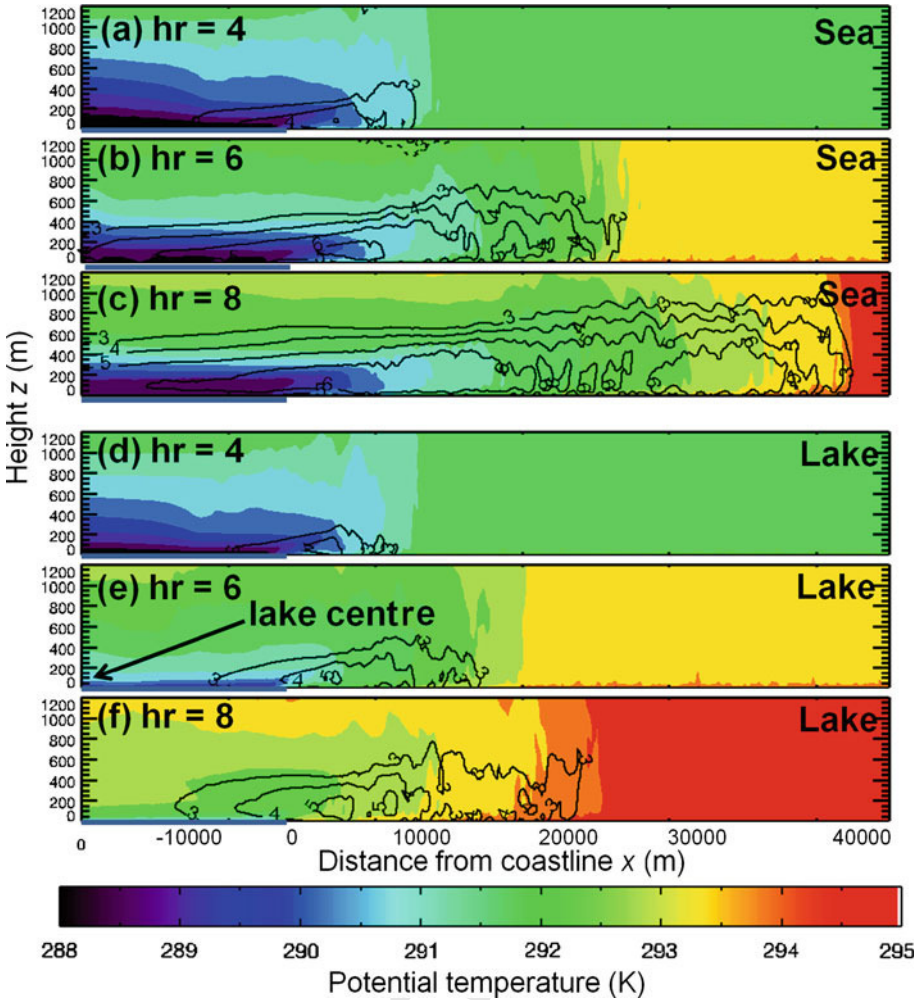


Fig. 9 Vertical cross-sections of the y -averaged low-level component of the sea-breeze circulation for the HI_H simulation for **a–c** the sea-breeze case and **d–f** 25 km diameter lake breeze at **a** and **d** hr 4, **b** and **e** hr 6, and **c** and **f** hr 8 (time is hours after simulation start, i.e., sunrise). Colours represent the potential temperature (θ , K) and *solid contours* outline cross-coast wind speed (u , m s^{-1}) greater than 3 m s^{-1} . The sea or lake surfaces are represented by *solid blue lines*

341 $\approx 4 \text{ K}$ between mid-morning and mid-afternoon results in a temperature difference between
 342 the air above the lake and land surfaces of $\approx 3.5 \text{ K}$, roughly half the horizontal temperature
 343 difference between the air above the land and the sea. Consequently, the mid-afternoon
 344 sea-breeze low-level onshore flow is enhanced both in its horizontal extent (the sea-breeze
 345 inland extent is roughly three times the lake-breeze inland extent) and wind speed relative
 346 to the lake breeze (Fig. 9c, f). The similar magnitude of the horizontal temperature gradient
 347 at mid-morning for sea and lake breezes explains why the morning development is similar
 348 for both lake and sea breezes, as the heating is not yet sufficient to deplete the cool lake
 349 air. The maximum horizontal temperature gradient and associated low-level onshore flow
 350 occurs immediately inland from the coast for a lake breeze. Consequently, boundary-layer

Idealized Large-Eddy Simulations of Sea and Lake Breezes

351 convection and the resultant turbulent frontolysis acting on the smaller horizontal tempera-
352 ture gradient associated with the lake-breeze onshore low-level flow reduces the afternoon
353 inland penetration of the lake-breeze front compared to the sea-breeze front (Figs. 5c, d; 9).

354 Another difference noted between lake and sea breezes is that the lake-breeze horizontal
355 wind speeds fluctuate more in time than do the sea-breeze horizontal wind speeds (Fig. 5a, b).
356 These fluctuations are observed to be associated with periodic weakening and strengthening
357 of the horizontal temperature gradient, similar to that described by Bastin and Drobinski
358 (2005) for a sea breeze. These fluctuations appear to be magnified by the limited amount of
359 cool air available over the smallest lakes.

360 The rate of depletion of the cool lake air for small and medium-sized lakes is modulated
361 by the magnitude of the heat flux. Specifying a higher heat flux leads to the lake breeze
362 consuming the available cool air more rapidly. Consequently, the mid-afternoon land-water
363 temperature difference for high values of the heat flux remains similar to the temperature
364 gradient observed for a low heat flux for small lake breezes (Fig. 3c, d). This modulation of
365 the rate of depletion (cold air rapidly depleted in the smallest lakes under a high heat flux)
366 is also hypothesized to be the reason that the difference in wind speed and inland extent
367 between small and large lake breezes is most pronounced in a high heat-flux environment
368 (Fig. 7d, e).

369 Finally, the decreased static stability of the low-level onshore flow for lake breezes versus
370 sea breezes (sea-breeze air is colder) is hypothesized to result in deeper lake breezes than
371 would be expected if the depth were simply scaled to decrease at a similar rate as the hori-
372 zontal wind speed and inland extent. Consequently, the lake-breeze depth is less sensitive to
373 changes in lake diameter than the horizontal wind speed and inland extent (Fig. 7c).

374 **4 Summary and Future Work**

375 Idealized numerical studies have been conducted on the sensitivity of sea and lake breezes to
376 variations in the heat flux and stability. Our analysis is the first to explore the effects of per-
377 turbations in the heat flux and stability on the spatio-temporal characteristics of lake breezes.
378 The results for sea breezes are generally consistent with prior scaling analyses and modelling
379 studies (Fig. 6). Similar to the results of Porson et al. (2007), the sea-breeze horizontal wind
380 speed and inland extent are largely controlled by the heat flux, while the sea-breeze depth is
381 controlled by stability and heat flux. The key conclusions of our study are as follows:

- 382 • horizontal asymmetries about the coast in the wind speeds associated with the sea-breeze
383 and lake-breeze onshore low-level flows are observed as a function of heat flux and
384 stability;
- 385 • the largest wind speeds within the lake-breeze low-level onshore flow are generally con-
386 fined immediately inland from the coast;
- 387 • lake-breeze circulations develop similarly to sea-breeze circulations through mid-morn-
388 ing but weaken significantly in the afternoon;
- 389 • there is no afternoon acceleration of the inland-moving lake-breeze front; hence, scal-
390 ing laws for lake breezes that capture the differing dynamics controlling lake-breeze
391 horizontal length scales is needed;
- 392 • lake-breeze circulations are less sensitive (more sensitive) to variations in heat flux (sta-
393 bility) than is the case for sea-breeze circulations;
- 394 • The lake-breeze and sea-breeze aspect ratios vary as a function of the heat flux and
395 stability.

396 The modelled dependence of sea and lake breezes on variations in the heat flux and sta-
397 bility has been presented in terms of simple metrics of sea and lake breezes: the vertical
398 depth and horizontal length and speed scales. However, there exists a plethora of additional
399 information within the LES that will necessitate more sophisticated analysis methods in the
400 future. Additional simulations remaining to be analyzed have also been conducted on the
401 sensitivity of sea and lake breezes to variations in the synoptic flow. Levy et al. (2011) find
402 a strong, persistent downdraft occurring within a sea breeze immediately onshore from the
403 coastline due to the combined effects of convergent horizontal rolls and synoptic flow. These
404 persistent downdrafts are not observed in the current LES with zero geostrophic flow, and
405 it will be interesting to determine whether the LES with non-zero geostrophic flow are able
406 to reproduce such downdrafts. In addition, future simulations will be conducted to ascertain
407 the sensitivity of small to medium-sized lake breezes to variations in the Coriolis parameter
408 and surface friction.

409 Future work will also require a scaling analysis of the simulations to contribute to current
410 sea-breeze scaling relations and to derive a scaling relation for lake breezes using approaches
411 similar to those for inland breezes (e.g., Drobinski and Dubos 2009; Hidalgo et al. 2010).
412 For sea breezes, developing scaling relations for the vertical wind speeds associated with the
413 sea-breeze front and return flow wind speeds and depth would likely be of interest to the
414 scientific community. However, the spatio-temporal variability of lake and sea breezes cap-
415 tured by these LES illustrates the need for new scaling estimates that include the sensitivity
416 to dependence on distance from the coast, time of day, and season as well as the difficulty to
417 describe these thermally-driven systems with simple scaling relations.

418 **Acknowledgments** This study was supported by the National Science Foundation project entitled "Lake
419 Breeze System of the Great Salt Lake" Grant # ATM-0802282. We appreciate the assistance provided by
420 Jimmy Dudhia, Rich Rotunno and Song-Lak Kang. An allocation of computer time from the Center for High
421 Performance Computing at the University of Utah is gratefully acknowledged. The help of two anonymous
422 reviewers is greatly appreciated in improving the paper.

423 References

- 424 Anthes RA (1984) Enhancement of convective precipitation by mesoscale variations in vegetative covering
425 in semiarid regions. *J Clim Appl Meteorol* 23:541–554
- 426 Antonelli M, Rotunno R (2007) Large-eddy simulation of the onset of the sea breeze. *J Atmos Sci* 64:4445–
427 4457
- 428 Baldi M, Dalu GA, Pielke RA (2008) Vertical velocities and available potential energy generated by landscape
429 variability—theory. *J Appl Meteorol Climatol* 47:397–410
- 430 Bastin S, Drobinski P (2005) Temperature and wind velocity oscillations along a gentle slope during sea breeze
431 events. *Boundary-Layer Meteorol* 114:573–594
- 432 Bastin S, Drobinski P (2006) Sea breeze induced mass transport over complex terrain in southeastern France:
433 a case study. *Q J Roy Meteorol Soc* 132:405–423
- 434 Catalano F, Moeng CH (2010) Large-eddy simulation of the daytime boundary layer in an idealized valley
435 using the Weather Research and Forecasting numerical model. *Boundary-Layer Meteorol* 137:49–75
- 436 Courault D, Drobinski P, Brunet Y, Lacarrere P, Talbot C (2007) Impact of surface heterogeneity on a buoy-
437 ancy-driven convective boundary layer in light winds. *Boundary-Layer Meteorol* 124:383–403
- 438 Crosman ET (2011) Idealized large-eddy simulation sensitivity studies of sea and lake breezes. Dissertation,
439 University of Utah, USA. <http://content.lib.utah.edu/u/?us-std3,20977>
- 440 Crosman ET, Horel JD (2010) Sea and lake breezes: a review of numerical studies. *Boundary-Layer Meteorol*
441 137:1–29
- 442 Dailey PS, Fovell RG (1999) Numerical simulation of the interaction between the sea breeze front and hori-
443 zontal convective rolls. Part I: Offshore ambient flow. *Mon Wea Rev* 127:858–878
- 444 Dalu GA, Pielke RA (1989) An analytical study of the sea breeze. *J Atmos Sci* 46:1815–1825

Idealized Large-Eddy Simulations of Sea and Lake Breezes

- 445 Drobinski P, Dubos T (2009) Linear breeze scaling: from large-scale land/sea-breezes to mesoscale inland
446 breezes. *Q J Roy Meteorol Soc* 135:1755–1766
- 447 Drobinski P, Bastin S, Dabas AM, Delville P, Reitebuch O (2006) Variability of the three-dimensional sea-
448 breeze structure in southeastern France: observations and evaluation of empirical scaling laws. *Ann*
449 *Geophys* 24:1783–1799
- 450 Fovell RG (2005) Convective initiation ahead of the sea breeze front. *Mon Wea Rev* 133:264–278
- 451 Fovell RG, Dailey PS (2001) Numerical simulation of the interaction between the sea breeze front and hori-
452 zontal convective rolls. Part II: Alongshore ambient flow. *Mon Wea Rev* 129:2057–2072
- 453 Garratt JR (1990) The internal boundary-layer—a review. *Boundary-Layer Meteorol* 50:171–203
- 454 Hidalgo J, Masson V, Gimeno-Presa L (2010) Scaling the daytime urban breeze circulation. *J Appl Meteorol*
455 *Climatol* 49:889–901
- 456 Hsu SA (1983) Measurements of the height of the convective surface boundary layer over an arid coast on the
457 Red Sea. *Boundary-Layer Meteorol* 26:391–396
- 458 Keen CS, Lyons WA (1978) Lake/land breeze circulations on the western shore of Lake Michigan. *J Appl*
459 *Meteorol* 17:1843–1855
- 460 Kniewel JC, Bryan GH, Hacker JP (2007) Explicit numerical diffusion in the WRF model. *Mon Wea Rev*
461 135:3808–3824
- 462 Levy I, Mahrer Y, Dayan U (2009) Coastal and synoptic recirculation affecting air pollutants dispersion: a
463 numerical study. *Atmos Environ* 43:1991–1999
- 464 Lundquist KA, Chow FK, Lundquist JK (2010) An immersed boundary method for the Weather Research and
465 Forecasting model. *Mon Wea Rev* 138:796–817
- 466 Miller STK, Keim BD, Talbot RW, Mao H (2003) Sea breeze: structure, forecasting and impacts. *Rev Geophys*
467 41:1–31
- 468 Mirocha JD, Lundquist JK, Kosović B (2010) Implementation of a nonlinear subfilter turbulence stress model
469 for large-eddy simulation in the Advanced Research WRF model. *Mon Wea Rev* 138:4212–4228
- 470 Moeng CH, Dudhia J, Klemp J, Sullivan P (2007) Examining two-way grid nesting for large-eddy simulation
471 of the PBL using the WRF model. *Mon Wea Rev* 135:2295–2311
- 472 Niino H (1987) The linear theory of land, and sea breeze circulation. *J Meteorol Soc Jpn* 65:901–920
- 473 Ogawa S, Sha W, Iwasaki T (2003) A numerical study of the interaction of a sea-breeze front with convective
474 cells in the daytime boundary layer. *J Meteorol Soc Jpn* 81:635–651
- 475 Papanastasiou DK, Melas D, Lissaridis I (2010) Study of wind field under sea breeze conditions; an application
476 of WRF model. *Atmos Res* 98:102–117
- 477 Patton EG, Sullivan PP, Moeng CH (2005) The influence of idealized heterogeneity on wet and dry planetary
478 boundary layers coupled to the land surface. *J Atmos Sci* 62:2078–2097
- 479 Physick WL (1980) Numerical experiments on the inland penetration of the sea breeze. *Q J Roy Meteorol Soc*
480 106:735–746
- 481 Porson A, Steyn DG, Schayes G (2007) Sea-breeze scaling from numerical model simulations, part I: pure
482 sea breezes. *Boundary-Layer Meteorol* 122:17–29
- 483 Rao PN, Fuelberg HE, Droegemeier KK (1999) High-resolution modeling of the Cape Canaveral area land-
484 water circulations and associated features. *Mon Wea Rev* 127:1808–1821
- 485 Reible DD, Simpson JE, Linden PF (1993) The sea breeze and gravity-current frontogenesis. *Q J Roy Meteorol*
486 *Soc* 119:1–16
- 487 Rotunno R, Chen Y, Wang W, Davis CA, Dudhia J, Holland GJ (2009) Large-eddy simulation of an idealized
488 tropical cyclone. *Bull Am Meteorol Soc* 90:1783–1788
- 489 Segal M, Leuthold M, Arritt RW, Anderson C, Shen J (1997) Small lake daytime breezes: some observational
490 and conceptual observations. *Bull Am Meteorol Soc* 78:1135–1147
- 491 Sha W, Kawamura T, Ueda H (1991) A numerical study on sea/land breezes as a gravity current: Kelvin-
492 Helmholtz billows and inland penetration of the sea-breeze front. *J Atmos Sci* 48:1649–1665
- 493 Sha W, Kawamura T, Ueda H (1993) A numerical study of nocturnal sea/land breezes: prefrontal gravity
494 waves in the compensating flow and inland penetration of the sea-breeze cutoff vortex. *J Atmos Sci*
495 50:1076–1088
- 496 Sha W, Ogawa S, Iwasaki T (2004) A numerical study on the nocturnal frontogenesis of the sea breeze front.
497 *J Meteorol Soc Jpn* 82:817–823
- 498 Simpson JE (1994) Sea breeze and local winds. Cambridge University Press, Cambridge
- 499 Skamarock WC, Klemp JB (2008) A time-split nonhydrostatic atmospheric model for weather research and
500 forecasting applications. *J Comput Phys* 227:3465–3485
- 501 Skamarock WC, Klemp JB, Dudhia J, Gill DO, Barker DM, Duda MG, Huang X-Y, Wang W, Powers JG
502 (2008) A description of the advanced research WRF version 3. NCAR/TN-475, 113 pp
- 503 Soler MR, Arasa R, Merino M, Olid M (2011) Modelling local sea-breeze flow and associated dispersion
504 patterns over a coastal area in north-east Spain: a case study. *Boundary-Layer Meteorol* 140:37–56

- 505 Steyn DG (1998) Scaling the vertical structure of sea breezes. *Boundary-Layer Meteorol* 86:505–524
506 Steyn DG (2003) Scaling the vertical structure of sea breezes revisited. *Boundary-Layer Meteorol* 107:177–
507 188
508 Tijn ABC, Van Delden AJ, Holtslag AAM (1999) The inland penetration of sea breezes. *Contrib Atmos Phys*
509 72:317–328

uncorrected proof